2017 21st International Conference on Process Control (PC)
June 6–9, 2017, Štrbské Pleso, Slovakia

Optimal Operation of Nanofilter Based Diafiltration Processes Using Experimental Permeation Models

Ayush Sharma*, Martin Jelemenský, and Miroslav Fikar
Faculty of Chemical and Food Technology
Slovak University of Technology in Bratislava
812 37 Bratislava, Slovakia
Email: {ayush.sharma, martin.jelemensky, miroslav.fikar}@stuba.sk

Radoslav Paulen
Process Dynamics and Operations Group
Technische Universität Dortmund
Dortmund, Germany
Email: radoslav.paulen@tu-dortmund.de

***Abstract*—In this paper, a choice of models for optimal control strategy is discussed for batch membrane processes. The system of lactose and salt in water is studied with the separation aim being concentration of lactose and simultaneous removal of salt. The most crucial part of the model is dependence of permeation rate on concentrations of components. Two models from literature and one data-based model are fitted to experimental data. An optimal control problem (OCP) is formulated to minimize processing time using diluant-to-permeate flow ratio as the control input. The optimal control strategy is found analytically and verified using numerical methods of dynamic optimization. The resulting processing times and the optimal input profiles are compared between all the models. Simulation case study confirms the attractiveness of the proposed approach.**

I. Introduction

Membranes act as a filter/sieve to separate, concentrate, remove, and clarify components from a liquid or gaseous mixture. They are established processing units in almost every industrial sector, especially in food, chemical, and bio technologies. Based on the component size, molecular weight and pressure, the membrane separation processes are divided into microfiltration (MF), ultrafiltration (UF), nanofiltration (NF), and reverse osmosis (RO). Nanofiltration processes retain molecules with molecular masses between 200-1000 g/mol. The operating pressure range for NF is 3-50 bar [1].

NF is used in a wide range of applications, including water softening, effluent water treatment, oil processing, beverage, dairy, and sugar industries [2]. In the production of lactose from dairy waste, for example, NF concentrates lactose molecules by retaining them on the solution side of the membrane while allowing salts to pass to the permeate side. The product, the concentrated lactose, is a commonly used material in the pharmaceutical industry as a carrier of drugs, e.g., in inhalations for asthma patients [3]. Besides pharmaceutical industry, lactose is emerging widely, in food and beverage industry, as a source for epilactose, galactooligosaccharides [4], lactitol, lactobionic acid, lactosucrose, lactulose, sialyllactose, and tagatose [5].

Diafiltration (DF) is a technique that uses MF, UF, and NF to eventually lower the concentration of impurities with the help of a diluant. In combination with NF, DF is applied to lower the concentration of salts [6].

This work studies modeling and optimal operation of NF with DF to increase the concentration of lactose and to reduce concentration of the salt. The modeling part focuses on characterization of the membrane permeation rate.

Generally, there are many factors influencing the permeation rate. The most important ones are concentration of solutes, temperature, and pressure. In our case, separation is conducted at constant temperature and pressure. So, the permeation rate basically depends on the concentration of solutes. [7] fitted permeate flow as an inverse polynomial function of albumin and ethanol, in order to concentrate albumin. [8] investigated resistance, gel-polarization, and osmotic pressure models. All these, and other modeling works done in past are mostly in the context of ultrafiltration, and not much of research has been done when it comes to modeling the permeation of NF with DF.

Modeling of NF to concentrate lactose was studied in [9]. In addition, no previous work describes an empirical relation and experimental models between the flow and concentration of lactose and NaCl [10]. Most of the works are based on existing theoretical models of e.g. film theory [11], or pore model, or diffusion model [12]. In a recent study of our group [13], permeation models with fouling from [14] were fitted to experimentally obtained data for the same solution, but the model neglected the effect of salt on the permeation rate.

This paper describes experimental procedure to obtain the permeation rate of NF with DF as a function of both lactose and salt. A model is developed to fit the experimental data. Additional empirical models studied from literature are also fitted for comparison. Then it is observed in a case study that the choice of the permeation model has only a very small influence on the time-optimal separation strategy. The results of optimization for each model are also compared to the traditional industrial strategy.

II. Process Description

A. Materials

Lactose monohydrate (M = 360.31 g/mol) and sodium chloride (M = 58.44 g/mol) manufactured by Centralchem (Slovakia) were used as solutes and reverse osmosis water was used as a solvent to prepare the experimental solution. The

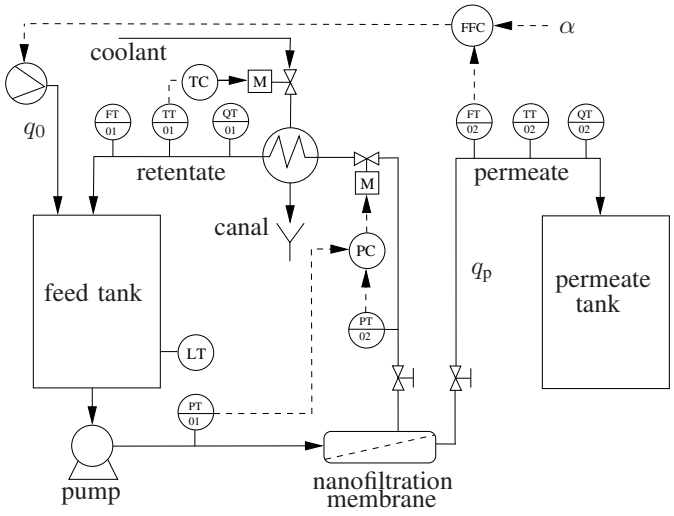

Fig. 1: Nanofiltration process scheme.

plant has a NFW-1812F nanofilter membrane manufactured by Synder Filtration, USA, with a cut-off range 300–500 Da, and a membrane area of $A = 0.465\,\mathrm{m}^2$.

B. Plant Description & Methods

The scheme of the nanofiltration plant is shown in Fig. 1. The batch starts with the addition of feed (of initial volume V_0) to the feed tank with initial concentrations of lactose and NaCl $c_{1,0}, c_{2,0}$, respectively. The pump then forces the feed towards the membrane in cross-flow mode, where the solution separates into two streams. The concentrated/rejected one is called retentate and comprises lactose and NaCl. The stream passing through the membrane is called permeate, and it basically comprises NaCl.

The transmembrane pressure (TMP) defined as,

$$\mathrm{TMP} = \frac{P_{\text{feed}} + P_{\text{retentate}}}{2} - P_{\text{permeate}} = 20\,\text{bar}, \tag{1}$$

is controlled at a constant value during the experiment. This control is achieved using a pressure controller (PC). The pressure could be changed by two actuators, i.e., the pump and the retentate side valve. The pumping rate is kept at a constant frequency to lower down wear and tear of the pump. Therefore, the retentate valve is used as the manipulated input. The temperature of the solution is maintained at a constant value of $26\,^\circ\mathrm{C}$ using a heat exchanger and a temperature controller (TC).

The diluant/water addition to perform DF is applied using another pump. This dilution rate is the input variable for this process and it is defined as

$$\alpha = \frac{q_0}{q_\mathrm{p}}, \tag{2}$$

where q_0 and q_p denote the inflow of the diluant into the feed tank and permeate flow from the membrane, respectively.

The classical control of batch DF mostly uses piece-wise constant α using three simple modes [7], [15]. These three modes can be written as

- No diluant input ($\alpha = 0$), i.e. concentration mode (C): the volume decreases, concentration of lactose increases, and concentration of NaCl stays constant.
- The diluant input rate equals the flow rate of permeate leaving the system ($\alpha = 1$), i.e. constant volume diafiltration mode (CVD): lactose concentration remains constant while NaCl concentration decreases.
- Diluant flow rate is less than the flow rate of permeate leaving the system ($0 < \alpha < 1$), i.e. variable volume diafiltration mode (VVD): volume decreases, lactose concentration increases, and NaCl concentration decreases.

In addition, [16], [17] have proposed two new basic modes:

- Dynamic volume diafiltration (DVD): α is not a constant but is varying with time ($0 < \alpha(t) < 1$).
- Pure dilution mode (D): a certain amount of diluant is instantaneously added to the solution. This can be symbolically represented by $\alpha = \infty$. Both lactose and NaCl concentrations decrease.

The concentration of NaCl (c_2) in the retentate is inferred from the conductivity measurements (sensor QT01), as the contribution of lactose to conductivity of the solution is negligible. The calibration curve obtained experimentally represents a linear model given as

$$c_2\,[\mathrm{g/L}] = 0.0007 \times \mathrm{QT}\,[\mu\mathrm{S/cm}] - 0.6949. \tag{3}$$

The concentration of lactose (c_1) is inferred from the mass balance in the feed tank using the level measurement from the plant (sensor LT). This method is described below.

C. Process Model

The standard model for a batch membrane process with two solutes can be described by three differential equations [17]

$$\frac{\mathrm{d}c_1}{\mathrm{d}t} = \frac{c_1 q_\mathrm{p}}{V}(R_1 - \alpha), \qquad c_1(0) = c_{1,0}, \tag{4a}$$

$$\frac{\mathrm{d}c_2}{\mathrm{d}t} = \frac{c_2 q_\mathrm{p}}{V}(R_2 - \alpha), \qquad c_2(0) = c_{2,0}, \tag{4b}$$

$$\frac{\mathrm{d}V}{\mathrm{d}t} = (\alpha - 1) q_\mathrm{p}, \qquad V(0) = V_0, \tag{4c}$$

where V is the actual volume in the feed tank and the constants R_1, R_2 are rejection coefficients of the respective solutes. These are dimensionless numbers in the interval $[0, 1]$. While $R = 0$ means that a solute passes through the membrane freely, $R = 1$ implies that the membrane blocks the solute and its concentration in the permeate is zero. Nanofilter membrane blocks lactose completely, hence $R_1 = 1$, which corresponds with the data from the membrane producer [18].

The value of $R_1 = 1$ therefore implies that the amount of lactose in the system remains constant and its concentration can be inferred from the actual volume, i.e.

$$c_1 V = c_{1,0} V_0 \quad \Rightarrow \quad c_1 = \frac{c_{1,0} V_0}{V}. \tag{5}$$

TABLE I: The initial and final conditions of the experiments.

experiment	1	2	3	4
$c_{1,0}$ [g/L]	42	40	41	51
$c_{2,0}$ [g/L]	4	3.5	6.5	4.5
$c_{1,\mathrm{f}}$ [g/L]	235	280	410	586
$c_{2,\mathrm{f}}$ [g/L]	0.8	1.6	1.3	0.8
V_0 [L]	30	30	30	34.5
V_f [L]	5.4	4.3	3	3

D. Experiments

In our recent work we have studied the effect of lactose concentration [13] on permeate flow rate with NF. In this paper we investigate influence of both solute (lactose, NaCl) concentrations on permeate flow rate. The experiments consist of the sequence of two modes: C-CVD.

The parameters of the experiments are shown in Table I and cover a range of typical conditions for this mixture. The results are shown in Figs. 2, 3. The flow was measured using the flow transmitter FT-02 on the permeate side.

The concentration mode can be characterized by the constant value of NaCl ($c_{2,0}$). Similarly, the switch to CVD mode can be recognized by the constant concentration of lactose in the second part of the experiment. The first fact implies that the rejection of NaCl by the membrane is zero, i.e. $R_2 = 0$ in (4b). The inverse relation between the concentration of lactose and permeation rate during the concentration mode is also clear from the figures. While the concentration of lactose increases, the permeate flow rate decreases. Similarly in the CVD step, the inverse relation between the concentration of NaCl and permeate flow rate can be inferred.

During CVD, the lactose concentration stays around a constant value, while the concentration of NaCl falls, and thus we see an increase in the permeate flow rate. This inverse relation can be attributed to viscous forces which increase with concentration and vice versa, and due to concentration polarization phenomenon [19].

E. Permeate Flow Modeling from Experimental Data

Based on above experiments, and from our previous results [13] it is clear that NF permeation rate depends on concentrations of both lactose and NaCl, i.e. $q_\mathrm{p} = q_\mathrm{p}(c_1, c_2)$. An experiment of nanofiltration (Fig. 4) to concentrate lactose from 50 [g/L] to 500 [g/L] was used to perform the fitting. 70 data points of concentrations were used to perform model fitting and parameter estimation. The sample time was 0.05 h, and in Fig. 4 samples after every 0.1 h are shown.

Various forms of models studied from literature and novel models were tried to fit the permeate flow rate as a function of lactose and NaCl concentration. These include the following:

- Exponential model: This model selection was based purely on the experimental data when compared among other structures, as it predicted well the permeate flow. It is given as

$$q_\mathrm{p} = \gamma_1 \mathrm{e}^{(\gamma_2 c_1)} + \gamma_3 c_2 + \gamma_4 c_1 c_2. \tag{6}$$

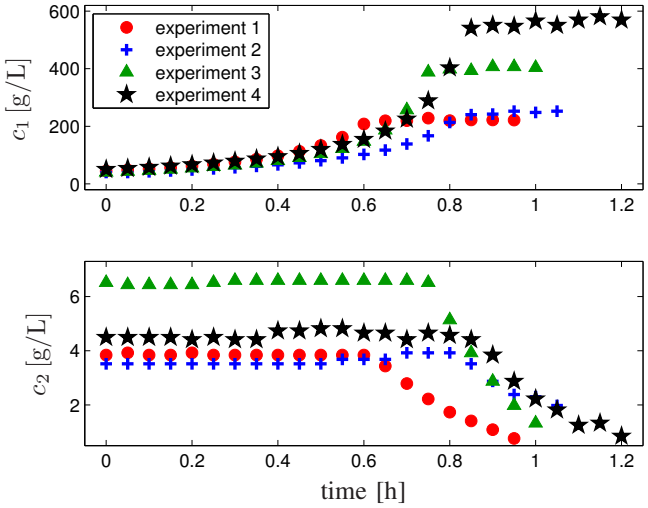

Fig. 2: Concentration measurements.

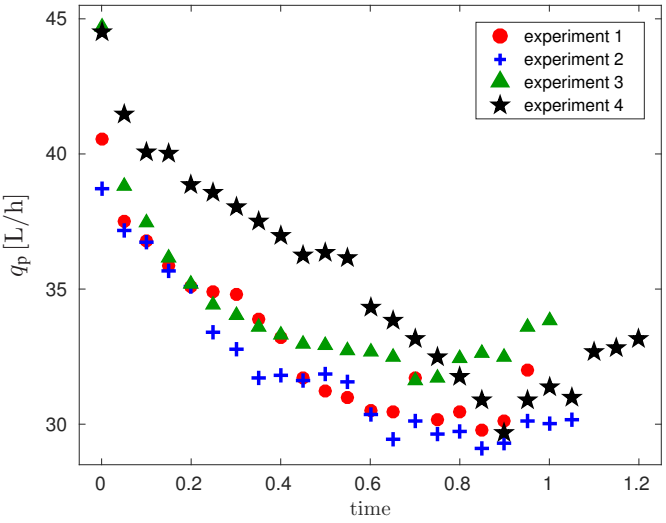

Fig. 3: Permeate flow rate measurements.

- Generalized limiting flux (GLF) model: This model has been taken from [20]. It can be written as

$$q_\mathrm{p} = \gamma_1 + \gamma_2 \ln(c_1) + \gamma_3 \ln(c_2). \tag{7}$$

- Inverse model: This model has been taken from [7]. It approximates the permeate flow rate by an inverse polynomial function of concentrations, i.e.

$$q_\mathrm{p} = \frac{1}{\gamma_1 + \gamma_2 c_1 + \gamma_3 c_2 + \gamma_4 c_1 c_2 + \gamma_5 c_1^2 + \gamma_6 c_2^2}. \tag{8}$$

The non-linear least-squares method was employed to get parameters $\gamma_1, \ldots, \gamma_6$ of all models. The resulting parameters are given in section VI and the corresponding permeate flows in Fig. 4. Experiments with larger set of data were also tested and same parameters were found. It can be observed that the exponential model fits the data better than the literature models. The value of sum of squared errors was also the

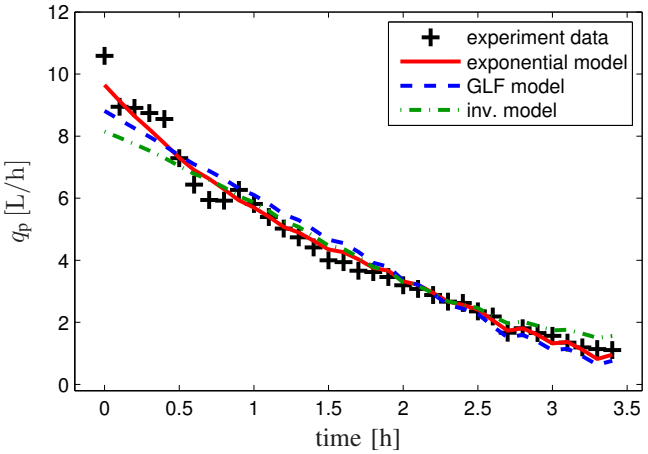

Fig. 4: Data of permeate flow rate from experiment, and the simulation of three estimated models.

minimum for exponential model, followed by GLF model, and the inverse model stood last among them.

Note that the fitting and estimation approach adopted in this work did not take into account time and is static, i.e. experimental flux and concentration data was used to estimate the expression $q_p(c_1, c_2)$. Another possible procedure would be dynamic approach when both concentration and flux would be used from model equations (4).

III. Process Optimization

The optimization goal is to find such time-dependent function $\alpha(t)$ which guarantees the transition from given initial $c_{1,0}, c_{2,0}$ to final $c_{1,f}, c_{2,f}$ concentrations in minimum time.

The optimization problem can be formulated as:

$$\mathcal{J}^* = \min_{\alpha(t)} \int_0^{t_f} 1 \, \mathrm{d}t, \tag{9a}$$

s.t.

$$\dot{c}_1 = c_1^2 \frac{q_p}{c_{1,0} V_0} (R_1 - \alpha), \tag{9b}$$

$$\dot{c}_2 = c_1 c_2 \frac{q_p}{c_{1,0} V_0} (R_2 - \alpha), \tag{9c}$$

$$c_1(0) = c_{1,0}, \qquad c_2(0) = c_{2,0}, \tag{9d}$$

$$c_1(t_f) = c_{1,f}, \qquad c_2(t_f) = c_{2,f}, \tag{9e}$$

$$q_p = (8), \text{ or } (7), \text{ or } (6) \tag{9f}$$

$$\alpha \in [0, \infty), \tag{9g}$$

where relation (5) is used to simplify the model. The problem was solved using both analytical and numerical tools.

The analytical approach is taken from [17]. According to theory, the optimal diluant addition strategy is a switching non-linear feedback control, consisting of three arcs. The first and the third one are on the input boundaries, while the middle one is derived from the singular arc, i.e.

$$S = q_p + \frac{\partial q_p}{\partial c_1} c_1 + \frac{\partial q_p}{\partial c_2} c_2 = 0. \tag{10}$$

The equation $S = 0$ marks the switching condition from minimum/maximum input to the input implemented during the singular arc, and this input is written as [17]

$$\alpha_s = \frac{\frac{\partial S}{\partial c_1} c_1}{\frac{\partial S}{\partial c_1} c_1 + \frac{\partial S}{\partial c_2} c_2}. \tag{11}$$

The resulting S and α_s for each of the three models can be formulated as,

1) *Exponential model*:

$$S = 2\gamma_3 c_2 + \gamma_1 \mathrm{e}^{(\gamma_2 c_1)} + 3\gamma_4 c_1 c_2 + \gamma_1 \gamma_2 c_1 \mathrm{e}^{(\gamma_2 c_1)}, \tag{12}$$

$$\alpha_s = \frac{2\frac{\gamma_3}{c_1} + 18\gamma_4 + 5\frac{\gamma_1 \gamma_2^2 c_1}{c_2} \mathrm{e}^{(\gamma_2 c_1)} + 10\frac{\gamma_1 \gamma_2}{c_2} \mathrm{e}^{(\gamma_2 c_1)}}{5(2\frac{\gamma_3}{c_1} + 6\gamma_4 + \frac{\gamma_1 \gamma_2^2 c_1}{c_2} \mathrm{e}^{(\gamma_2 c_1)} + 2\frac{\gamma_1 \gamma_2}{c_2} \mathrm{e}^{(\gamma_2 c_1)})}. \tag{13}$$

2) *GLF model*:

$$S = q_p - \gamma_2 - \gamma_3, \tag{14}$$

$$\alpha_s = \frac{\gamma_2}{\gamma_2 + \gamma_3}. \tag{15}$$

3) *Inverse model*:

$$S = \gamma_1 - \gamma_5 c_1^2 - c_1 c_2 \gamma_4 - \gamma_6 c_2^2, \tag{16}$$

$$\alpha_s = \frac{0.5\gamma_4 c_1 c_2 + \gamma_5 c_1^2}{\gamma_5 c_1^2 + \gamma_4 c_1 c_2 + \gamma_6 c_2^2}. \tag{17}$$

It can interestingly be seen that although good estimation of γ_2 and γ_3 is required for fitting the data, these two parameters do not play any role and hence do not need very exact estimation in the context of optimization.

Numerical optimization (orthogonal collocations) was also used to solve the case for all models. DYNOPT toolbox [21], implemented in MATLAB programming environment, was used to perform this optimization. The control trajectory was divided into three discontinuous segments. Five collocation points in case of states, one in case of control input, were found to be enough to find the optimal solution.

IV. Optimization Results

The aim is to drive the concentration of lactose from $c_{1,0} = 40$ g/L to $c_{1,f} = 120$ g/L, and simultaneously to reduce the concentration of NaCl from $c_{2,0} = 3.25$ g/L to $c_{2,f} = 1$ g/L. The initial volume V_0 is 30 L.

The traditional approaches that can accomplish the same objective include C-CVD and VVD modes of operation. Only the first one was applied, the second one based on simulation results was clearly ineffective and unsuitable in context of the desired reduction of processing time.

The time-optimal strategy for given initial and final conditions consists of three modes:

1) Concentration mode with minimum input $\alpha = 0$, till $S = 0$ condition is met.
2) The input in the second step should be the singular control, hence $\alpha = \alpha_s$. The singular control is maintained till the condition $c_1/c_2 = c_{1,f}/c_{2,f}$ is met.

3) The third step is dilution mode with $\alpha = \infty$, till we reach the final concentrations.

The results are shown in Figs. 5 and 6. The concentration profile for all models and strategies is shown in Fig. 5. Similarly, the time-optimal input profile for all models, along with the traditional input strategy of C-CVD for inverse model can be seen in Fig. 6. The simulations with exponential, GLF, and inverse models assume that the process and the model are the same.

The time-optimal operation strategy for exponential and GLF model was found to be a sequence of C-VVD-D modes, i.e. the singular control given by expressions (13), (15) was within the concentration range constant $\alpha_s = 1.02$ and $\alpha_s = 0.96$, respectively. The time-optimal strategy for inverse model was a sequence of C-CVD-D modes where the singular control in the second step given by (17) for given concentrations and parameter values was equal to $\alpha_s = 1$.

Identical strategy was found also by the numerical method of orthogonal collocations. There, we assumed that the second step was CVD ($\alpha_s = 1$) for all three models. We have found that the final time was almost identical for both analytical and numerical techniques. Hence, the second step for all three models can be replaced with CVD step, without any significant loss of optimality.

Note that even if the modeled permeate fluxes are similar, accumulated differences resulted in seemingly similar state trajectories for GLF and inverse models (Fig. 5) with different optimal controls and with different final processing times (Fig. 6). This shows that the model should be accurate in a large operating region.

The traditional approach ends at the final desired concentrations in two steps. The concentration (C) mode is applied in the first step until $c_{1,\mathrm{f}}$ is reached. Then, CVD mode is applied to reduce the concentration of the second component till $c_{2,\mathrm{f}}$

As the time-optimal control over-concentrates the solution until the condition of $c_{1,\mathrm{f}}/c_{2,\mathrm{f}}$ is met, the third step is dilution mode (upward arrows in Fig. 6), i.e. the filtration stops and the required volume of diluant is added to get the final desired concentrations.

Table II compares the final processing times of all strategies assuming also model mismatch. The rows denote the model used as the controlled process whereas columns specify control strategy applied: either traditional C-CVD or one of the optimal ones.

It is evident that for all of the models the proposed time-optimal strategy performs better than traditional one – the final time of C-CVD is always the largest in every row. The table also provides a degree of sub-optimality when time optimal results of one model are applied to different process. It can be seen from the values that even though process mismatch resulted in some loss of optimality, it was still better than the traditional C-CVD approach. The difference between the optimal time taken with different models was not very significant in case of GLF and inverse models; while it was 6.6% for exponential model. The time required by the optimal strategy was about 10% less than its traditional counterpart

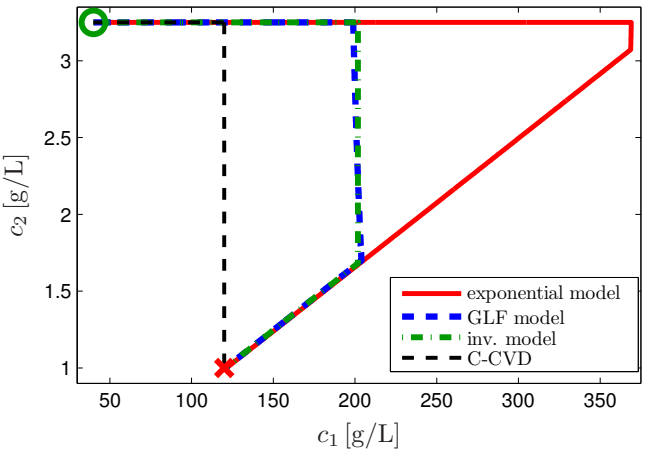

Fig. 5: State concentration diagram for different models.

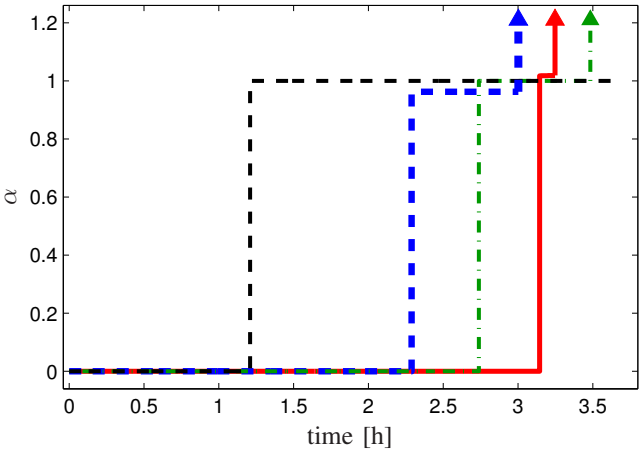

Fig. 6: Time optimal input for different models.

TABLE II: Comparison of processing times

	C-CVD [h]	optimal [h] (exp.)	optimal [h] (GLF)	optimal [h] (inv.)
exponential	3.60	3.25	3.52	3.48
GLF	3.12	3.08	3.00	3.02
inverse	3.64	3.53	3.49	3.48

for exponential model, and for GLF and inverse model this reduction in time with the time-optimal strategy was about 4% and 5%, respectively. The major reason for difference between traditional and time-optimal strategies is the step to reduce the concentration of NaCl. It was observed in the experiments and in the simulations that the time required to concentrate lactose in C mode is much shorter than the time required to decrease the concentration of NaCl using CVD or VVD mode.

V. Conclusions

We studied time-optimal operation of nanofiltration processes in order to concentrate lactose and reduce NaCl. Based

on the experiments with the solutes, a permeate flow rate model was developed and verified using experimental data. In addition, two other models studied from literature were fitted to the experimental data using simple static relations. The optimal control problem was then formulated to minimize the time of operation. The solution was found by employing the analytical solution from an earlier work using Pontryagin's minimum principle and it was confirmed by numerical method of orthogonal collocation.

The presented approach was then tested on a simulation case study. The time-optimal control strategy consisted of three steps, i.e. bang-bang on the boundaries and singular control as the middle step. The performance of this time-optimal control strategy was compared with traditional two step C-CVD strategy. The results show that the proposed approach is about $4 - 10\,\%$ faster than the traditional one.

It was also observed that the various experimentally chosen permeate flow models had minor effects on structure of the optimal process operation. On the other hand, a high quality model that covers a large concentration region could improve quality of the operation.

ACKNOWLEDGMENT

The authors gratefully acknowledge the contribution of the Slovak Research and Development Agency under the project APVV 15-0007 and the Scientific Grant Agency of the Slovak Republic (project 1/0004/17). This contribution/publication is also the partial result of the Research & Development Operational Programme for the project University Scientific Park STU in Bratislava, ITMS 26240220084, supported by the Research 7 Development Operational Programme funded by the ERDF.

REFERENCES

[1] G. Artuğ, *Modelling and Simulation of Nanofiltration Membranes*. Cuvillier, 2007.

[2] F. Salehi, "Current and future applications for nanofiltration technology in the food processing," *Food and Bioproducts Processing*, vol. 92, no. 2, pp. 161 – 177, 2014.

[3] R. Boerefijn, Z. Ning, and M. Ghadiri, "Disintegration of weak lactose agglomerates for inhalation applications," *International Journal of Pharmaceutics*, vol. 172, no. 12, pp. 199 – 209, 1998.

[4] B. Verasztó, A. Sharma, Q. D. Nguyen, G. Vatai, P. Czermak, and Z. Kovács, "Membrane filtration technology for processing whey and converting whey-based lactose into galactooligosaccharides," in *Conference Proceeding of the 6th Membrane Conference of Visegrad Countries*, J. Krzysztoforski and M. Szwast, Eds. Warsaw, Poland: Polish Membrane Society, 2013, p. E5.

[5] L.-F. Gutiérrez, S. Hamoudi, and K. Belkacemi, "Lactobionic acid: A high value-added lactose derivative for food and pharmaceutical applications," *International Dairy Journal*, vol. 26, no. 2, pp. 103 – 111, 2012.

[6] N. Yin, G. Yang, Z. Zhong, and W. Xing, "Separation of ammonium salts from coking wastewater with nanofiltration combined with diafiltration," *Desalination*, vol. 268, no. 13, pp. 233 – 237, 2011.

[7] M. Jaffrin and J. Charrier, "Optimization of ultrafiltration and diafiltration processes for albumin production," *Journal of Membrane Science*, vol. 97, pp. 71 – 81, 1994.

[8] G. van den Berg and C. Smolders, "Flux decline in ultrafiltration processes," *Desalination*, vol. 77, pp. 101 – 133, 1990.

[9] E. Suárez, A. Lobo, S. Álvarez, F. A. Riera, and R. Álvarez, "Partial demineralization of whey and milk ultrafiltration permeate by nanofiltration at pilot-plant scale," *Desalination*, vol. 198, no. 1, pp. 274 – 281, 2006.

[10] N. Hilal, H. Al-Zoubi, N. A. Darwish, A. W. Mohamma, and M. A. Arabi, "A comprehensive review of nanofiltration membranes: Treatment, pretreatment, modelling, and atomic force microscopy," *Desalination*, vol. 170, no. 3, pp. 281 – 308, 2004.

[11] R. Wang, Y. Li, J. Wang, G. You, C. Cai, and B. H. Chen, "Modeling the permeate flux and rejection of nanofiltration membrane separation with high concentration uncharged aqueous solutions," *Desalination*, vol. 299, pp. 44 – 49, 2012.

[12] D. Fierro, A. B. de Fierro, and V. Abetz, "The solution-diffusion with imperfections model as a method to understand organic solvent nanofiltration of multicomponent systems," *Journal of Membrane Science*, vol. 413414, pp. 91 – 101, 2012.

[13] A. Sharma, M. Jelemenský, R. Paulen, and M. Fikar, "Estimation of membrane fouling parameters for concentrating lactose using nanofiltration," in *26th European Symposium on Computer Aided Process Engineering*, vol. 26. Portorož, Slovenia: Elsevier B.V., 2016, pp. 151–156.

[14] J. Hermia, "Constant pressure blocking filtration laws-application to power-law non-Newtonian fluids," *Transactions of the Institution of Chemical Engineers*, vol. 60, no. 2, pp. 183 – 187, 1982.

[15] G. Foley, "Water usage in variable volume diafiltration: comparison with ultrafiltration and constant volume diafiltration," *Desalination*, vol. 196, pp. 160 – 163, 2006.

[16] H. Lutz, *Ultrafiltration for Bioprocessing*. Woodhead Publishing, 2015.

[17] R. Paulen and M. Fikar, *Optimal Operation of Batch Membrane Processes*. Springer, 2016.

[18] Synder, "Nanofiltration membrane elements," Synder Sanitory Catalog 2014 - Synder Filtration, pp. 7 –8, 2014.

[19] S. Bhattacharjee, J. C. Chen, and M. Elimelech, "Coupled model of concentration polarization and pore transport in crossflow nanofiltration," *AIChE Journal*, vol. 47, no. 12, pp. 2733 – 2745, 2001.

[20] N. Rajagopalan and M. Cheryan, "Process optimization in ultrafiltration: Flux-time considerations in the purification of macromolecules," *Chemical Engineering Communications*, vol. 106, no. 1, pp. 57–69, 1991.

[21] M. Čižniar, M. Fikar, and M. A. Latifi, "MATLAB dynamic optimisation code dynopt. User's guide," KIRP FCHPT STU, Bratislava, 2006. [Online]. Available: https://bitbucket.org/dynopt

VI. APPENDIX

Parameters for the three models presented and fitted in section II-E are listed here.

A. Exponential model

γ_1	34.999999999999979
γ_2	-0.019600000000022
γ_3	1.593108283198708
γ_4	-0.002833952404820

B. GLF model

γ_1	34.505554919850738
γ_2	-5.410609785568382
γ_3	-0.210358558294745

C. Inverse model

γ_1	0.095000000000022
γ_2	0.000000000000022
γ_3	0.000000000000022
γ_4	0.000000000000022
γ_5	0.000002333865682
γ_6	0.000000000000022